Probing defects in Al–Mg–Si alloys using muon spin relaxation

Sigurd Wenner* and Randi Holmestad
Department of Physics, NTNU, Høgskoleringen 5, Trondheim NO-7491, Norway

Kenji Matsuda and Katsuhiko Nishimura
Department of Materials Science and Engineering, University of Toyama, Gofuku 3190, Toyama-shi, Toyama 930-8555, Japan

Teiichiro Matsuzaki and Dai Tomono
Advanced Meson Science Laboratory, RIKEN Nishina Center for Accelerator Based Science, RIKEN, Wako, Saitama 351-0198, Japan

Francis L. Pratt
ISIS Facility, Rutherford Appleton Laboratory, Chilton OX11 0QX, UK

Calin D. Marioara
Materials and Chemistry, SINTEF, Box 4760 Sluppen, Trondheim NO-7465, Norway
(Dated: August 24, 2012)

Muon spin methods are very sensitive to nanoscale defects such as trace elements and vacancies in metals. This sensitivity is required when investigating Al–Mg–Si alloys, a complicated system in which diffusion-controlled phase transformations are responsible for the most important hardening mechanisms. We present muon spin relaxation experiments conducted on Al–Mg–Si alloys at measurement temperatures in the range 20–300 K. Varying the alloy composition and heat treatment, we find differences in muon depolarization in several temperature regimes. This reflects differences in concentration of several types of muon-trapping defects. We identify free solute atom and vacancy regimes, and confirm that the concentration of these defects decrease when an alloy is annealed at low temperature. We further attribute one regime to Mg–Si–vacancy clustering, a mechanism required for precipitation hardening during aging. After storage at room temperature, muon trapping in this regime is more pronounced for a Mg-rich alloy than a Mg–Si-balanced alloy.

I. INTRODUCTION

Muon spin methods have been used for probing the microscopic properties of a wide range of materials, including superconducting and magnetic materials,[1–3] biological molecules,[4] and semiconductors.[5,6] Most of the research activity using muons on aluminium and other pure metals took place in the late 1970s and early 1980s.[7–9] In non-magnetic materials, polarized positive muons (μ^+) can be used as probes for atomic-scale magnetic fields. The methods have been proven very sensitive to point defects such as trace element atoms.[8,10] The property of muons known as *asymmetric decay* is central to how the measurements are conducted: Muons are unstable, and decay to positrons, whose directions of motion tend to be parallel to the muon spin. The detection of these positrons enables us to follow the time evolution of the average muon polarization inside the material. In this paper, the acronym µSR refers to *muon spin relaxation*, with which no external magnetic field is applied.

Aluminium alloys containing Mg and Si as main alloying elements ($6xxx$ series alloys) are used extensively as structural materials due to their formability, mechanical strength, and corrosion resistance. These alloys are heat-treatable, which means that their microstructure changes when thermal and mechanical treatment is applied to them. Typically, $6xxx$ alloys are given a solution heat treatment (SHT) before subsequent aging, to distribute the solute elements evenly in the Al matrix, and to introduce a high concentration of vacancies, which is necessary for later substitutional diffusion of the solute elements. A unique feature of Al–Mg–Si alloys is that room temperature (RT) storage between SHT and artificial aging (AA) at higher temperatures has a significant effect on the hardness of the material.[11,12] This effect is called *natural aging* (NA), and can degrade the mechanical properties of dense alloys (with solute content above 1%).[11,13] NA is caused by the clustering of solute atoms.[14,15] Upon aging above $\approx 150°C$, metastable phases with well-defined crystal structures precipitate in the Al matrix.[16] The processes of clustering and precipitation are very sensitive to parameters such as alloy composition, storage time, aging temperature, and heating/cooling rates.

We have applied µSR to samples of Al–Mg–Si alloys with various compositions and heat treatments. The evolution of the muon polarization is measured at a range of temperatures, as the trapping of muons by nanometer-sized defects is temperature-dependent. This enables the estimation of properties of several types of defects as averaged over a macroscopic volume of the material under study. To our knowledge, measurements of this kind have not before been conducted on aluminium alloys.

This paper presents results from µSR studies of alloys with typical industrial Mg- and Si-content. Section II re-

views the theoretical background of µSR and muon diffusion in non-magnetic materials. Section III gives the experimental methodology as well as the compositions and heat treatments of the samples. In section IV we explain how the experimental data is treated and introduce the simulations used to estimate quantities associated with muon diffusion. The results of these estimations are presented in section V, while sections VI and VII are dedicated to discussion and summary of the central findings.

II. THEORY OF µSR

When a spin-polarized high energy muon enters a metallic solid, inelastic scattering processes quickly reduce its energy to a thermal level, while retaining the muon spin. In analogy with hydrogen atoms, muons occupy interstitial sites in metals. The magnetic field at the muon site causes Larmor precession of the muon spin. In the absence of an external field, the precession is induced exclusively by small (~ 1 mT) local magnetic fields inside the material. The dynamics of µSR can be decoupled into spin relaxation (depolarization) by these fields and muon diffusion.

An atomic nucleus sets up the dipole field[17]

$$\mathbf{B}(\mathbf{m},\mathbf{r}) = \frac{\mu_0}{4\pi r^3}\left[3(\mathbf{m}\cdot\hat{\mathbf{r}})\hat{\mathbf{r}} - \mathbf{m}\right], \tag{1}$$

where $\mathbf{m}$ is the magnetic moment of the nucleus, $\hat{\mathbf{r}}$ is a unit vector pointing from the muon to the nucleus, and μ_0 is the electrical permittivity of vacuum. There are other sources to local magnetic field contributions inside metals, such as the quadrupole moment of nuclei and both core and conduction electrons.[17] Inside a diamagnetic material, the total field from electrons gives spin relaxation times longer than 100 μs, which is much greater than the lifetime of a muon.[17,18] The nuclear dipole moments are thus the greatest contributions.

A positive muon has an average lifetime of 2.197 μs. Its main decay channel produces one positron and two neutrinos through an asymmetric decay. The probability for the positron to be emitted at an angle θ from the muon spin is

$$p(\theta) = 1 + A\cos\theta, \tag{2}$$

with A being the asymmetry of the decay, which depends on the energy of the emitted positron. In experiments, $A \approx 0.25$ is normally measured. In the present µSR experiments, muons are polarized antiparallel to their direction of motion. Two detectors are placed in the forward (parallel to the initial polarization) and backward direction, and the positron counts, N_f and N_b, are measured at a range of times t after muon implantation. From this we find the muon spin asymmetry $G(t)$, often expressed through the longitudinal *relaxation function* $g(t)$,

$$G(t) = Ag(t) = \frac{N_\mathrm{f} - \alpha N_\mathrm{b}}{N_\mathrm{f} + \alpha N_\mathrm{b}}. \tag{3}$$

The parameter α compensates for differences in distance between the sample and the two detectors.

The Kubo–Toyabe (KT) model[19] gives a simple and often accurate picture of the dynamics of µSR. The model assumes a Gaussian distributed magnetic field at the muon site. Averaging over an ensemble of muons with an exponentially distributed lifetime, one obtains the static KT relaxation function,

$$g^\mathrm{KT}(t) = \frac{1}{3} + \frac{2}{3}\left(1 - \Delta^2 t^2\right)\exp\left(-\frac{1}{2}\Delta^2 t^2\right), \tag{4}$$

where we have introduced the *dipolar width* $\Delta = \gamma_\mu B_\mathrm{RMS}$, a product of the gyromagnetic ratio of the muon $\gamma_\mu = 8.5168 \times 10^8\ \mathrm{T^{-1}s^{-1}}$ and the root–mean–square magnetic field strength B_RMS. The effect of diffusion on $g(t)$ is an important one, as *motional narrowing*[17] of the field distribution decreases the depolarization rate. At temperatures above ~ 1 K, the muon diffuses interstitially by a phonon-assisted tunneling process.[17] This is well described by the strong-collision model, in which muon jumps happen instantly and the magnetic field is uncorrelated between adjacent interstitial sites.[18] This leads to the dynamic KT relaxation function, computed by solving an integral equation.[20] Faster dynamics will shift the KT minimum to longer times.[21] In the limit of fast diffusion, this function can be approximated by

$$g^\mathrm{DKT}(t) \approx \exp\left(-\frac{2\Delta^2}{\nu}t\right), \tag{5}$$

where ν is the muon hopping rate. In certain circumstances, Δ^2/ν is so small for freely diffusing muons that the depolarization becomes negligible.[10]

Trapping by lattice defects can prevent muons from diffusing, introducing another complication to the dynamics. The fraction of time a muon spends trapped inside the material, f_t, will greatly influence $g(t)$. We have derived this quantity from a two-state stochastic trapping–detrapping model. When averaged over the lifetime of a muon, the trapped time fraction becomes

$$f_\mathrm{t} = \frac{\nu_\mathrm{t}}{\nu_\mathrm{t} + \nu_\mathrm{d}} - \left(\frac{\nu_\mathrm{t}}{\nu_\mathrm{t} + \nu_\mathrm{d}} - p_0\right)\frac{\lambda}{\nu_\mathrm{t} + \nu_\mathrm{d} + \lambda}, \tag{6}$$

where ν_t, ν_d, and λ are the (constant) trapping, detrapping, and decay rates, and p_0 is the fraction of initially trapped muons. From the theory of diffusion-controlled trapping, we have that ν_t is proportional to the concentration of muon-trapping defects,[22] while ν_d depends on how tightly the muon is bound to the defects. The equilibrium trapped time fraction (for muons of infinite lifetime) would be $\nu_\mathrm{t}/(\nu_\mathrm{t} + \nu_\mathrm{d})$.

Inside a material analyzed by µSR, the concentration of muons is extremely low at all times. Muons behave as light protons in Al, and are expected to have a negligible influence on the diffusion of vacancies and solute atoms during experiments of any duration. In non-metallic materials, bound muon–electron systems (muonium) have been used as a model for hydrogen atoms with accompanying diffusion and bonding properties.[5,6,23]

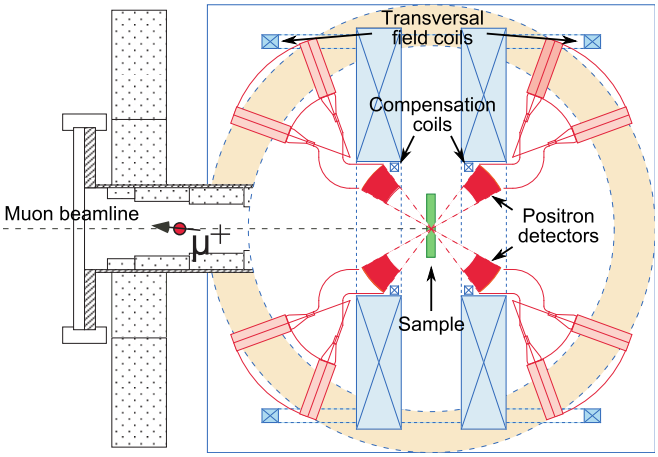

FIG. 1. (Color online) The experimental setup, showing the ARGUS muon spectrometer and a spin-polarized muon beam entering from the left.

TABLE I. The conditions studied by temperature series µSR measurements. Composition (atomic fraction, remainder is Al) and heat treatment after SHT is shown. RT means room temperature, `AQ` denotes "as-quenched".

Composition	Heat treatment	Short name
1.07% Mg, 0.53% Si	≈ 15 min @ RT	`1.6-AQ`
”	15 days @ RT	`1.6-15d`
”	163 days @ RT	`1.6-163d`
”	1000 min @ 70°C	`1.6-70C`
”	1000 min @ 100°C	`1.6-100C`
”	1000 min @ 200°C	`1.6-200C`
0.67% Mg, 0.33% Si	≈ 77 min @ RT	`1.0-AQ`
”	1000 min @ 70°C	`1.0-70C`
0.67% Mg, 0.77% Si	≈ 15 min @ RT	`1.4B-AQ`
”	163 days @ RT	`1.4B-163d`
”	1000 min @ 70°C	`1.4B-70C`
0.01% Trace elements	66 days @ RT	`pure`

III. EXPERIMENTAL

The µSR experiments were conducted at the RIKEN-RAL Muon Facility in Oxfordshire, UK.[24] Its pulsed muon beamline provides a high intensity which gives about 1 million positron counts per minute. Figure 1 shows a schematic of the muon spectrometer. Compensation coils surrounding the sample are used to counter the magnetic field of the Earth and the last quadrupole magnet in the muon beamline. The residual field is $\sim 5\ \mu$T, well below the magnitude of typical local fields in Al, $\sim 1000\ \mu$T. The annular forward and backward detector arrays each have a 25% solid angle coverage. For each sample, the α parameter in Eq. (3) was estimated by *muon spin rotation* experiments using external transversal fields of 2.0–3.0 mT.

The samples used were of pure aluminium (99.99%) and three different ultra-pure Al–Mg–Si alloys. Two of the alloys had an Mg/Si ratio of 2 and total atomic solute 1.6% and 1.0%, while the third alloy was Mg–Si-balanced and contained a total of 1.4% solutes. Many industrial $6xxx$ alloys contain comparable amounts of Mg and Si, with Fe, Mn, Cu, and other elements added in smaller amounts. All samples were given a SHT at 575°C for 1 hour, ensuring an even distribution of solutes in solid solution. We quenched the samples in ice water before directly applying further heat treatments. Table I summarizes the conditions of the 11 samples used. Similar conditions have been studied extensively using various characterization methods such as atom probe tomography (APT),[25] positron annihilation spectroscopy (PAS),[26] and transmission electron microscopy (TEM).[27,28] Their microstructures are therefore well-known.

The muon spin relaxation functions were obtained while keeping the samples at fixed temperatures with a helium cryostat. The samples were cooled down to 20 K (5 K for pure Al) and heated in steps up to 300 K. At each measurement temperature, 20–60 million positron counts were recorded.

IV. DATA ANALYSIS AND SIMULATIONS

The programs WIMDA[29] and MATLAB were used for µSR data analysis. The measurement error $\epsilon(t)$ in the relaxation functions was estimated by assuming that the number of detected muons in each time bin follow a Poisson distribution. To get an overview of the temperature dependence of the muon behavior, the experimental relaxation functions were fitted to a Gaussian,

$$G(t) = a \exp\left(-\frac{1}{2}\sigma^2 t^2\right) + b. \tag{7}$$

The parameter σ gives a good measure of the muon depolarization rate. Not all relaxation functions are well described by a Gaussian, but it gives a consistent fit using only one non-linear parameter. When a KT fit is attempted, the Δ parameter has a temperature dependence very similar to that of σ.

To better understand the physics behind the experimental relaxation functions, we simulate the diffusion, trapping, spin precession, and decay of muons using a Monte Carlo (MC) algorithm. The algorithm simulates random muons one by one, and unavoidably produces relaxation functions with statistical fluctuations similar to those observed in experiments. Although slower than KT-related integral equation methods, a MC simulation is more flexible, gives better control of the applied approximations, and produces more readily interpretable results.

The preferred muon sites in Al are tetrahedral at temperatures above ≈ 15 K.[30] Only Al nuclei generate considerable dipole fields, about 40 times stronger than those

of Mg and Si.[31] By using Eq. (1) to estimate the magnetic fields, we find that stationary muons in a perfect aluminium lattice give a dipolar width of $\Delta_{\mathrm{dipol}} = 0.495\ \mu\mathrm{s}^{-1}$. The experimental data cannot be reproduced by fixing Δ to this value as it makes the muon depolarization too fast. There can be two reasons for this: The simple dipole fields of Eq. (1) are not sufficient to describe the magnetic fields experienced by the muons, or the environments at the muon sites are significantly different from interstitial sites in pure Al. We have therefore resorted to the simpler approach of using a Gaussian magnetic field with an adjustable dipolar width Δ, as in the KT model.

Muon diffusion in Al has been shown to be very fast, even at temperatures below 1 K.[8] We can therefore assume that motional narrowing makes the spin relaxation negligible for muons in a free (non-trapped) state. This makes the muon diffusion rate ν superfluous as a simulation parameter. Trapping and detrapping by defects is described by the parameters ν_{t}, ν_{d}, and p_0, all defined below Eq. (6). In certain temperature ranges, several types of defects may act as muon traps simultaneously. The simulations use only a single trap, which is assumed to capture the average trapping behavior in such situations. When including Δ, our parameter set corresponds to the set used in an improved KT model by Hatano et al.[21] for Al–0.047% Mg. The results from this model and our MC simulation converge to the same values if the precision used in both models is increased sufficiently. We have generated a database of simulated relaxation functions by systematic variation of the four parameters. The decrease, recovery, and curvature of a relaxation function depends on all parameters in a complicated manner. Generally, higher values of Δ, ν_{t}, and p_0 make the depolarization faster, while a higher ν_{d} makes it slower.

The simulated functions are fitted to the experimental ones with a weighting function $\epsilon(t)^{-2}$. Because of the computational time the simulations require, the number of simulated relaxation functions have been limited to about 7000. The fitting parameters are thus varied with quite coarse steps. To account for this and increase the accuracy of the predicted physical quantities, we estimate the four parameters by weighted averages of all the simulated relaxation functions. The weights are given by E^{-2}, where E is the total error of fitting a simulated function to experimental data.

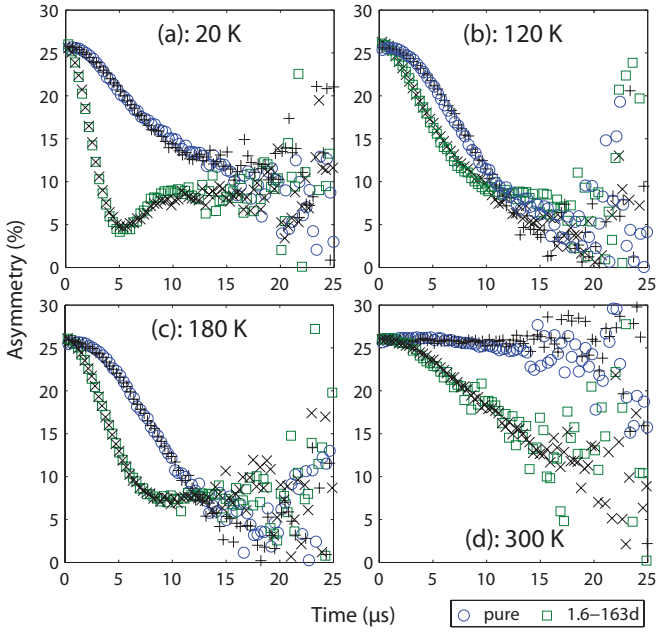

FIG. 2. (Color online) Experimental muon spin relaxation functions calculated from Eq. (3) at 4 selected temperatures for a room temperature stored alloy condition (`1.6-163d`) and pure Al. The best-fit simulated relaxation functions are shown as black crosses.

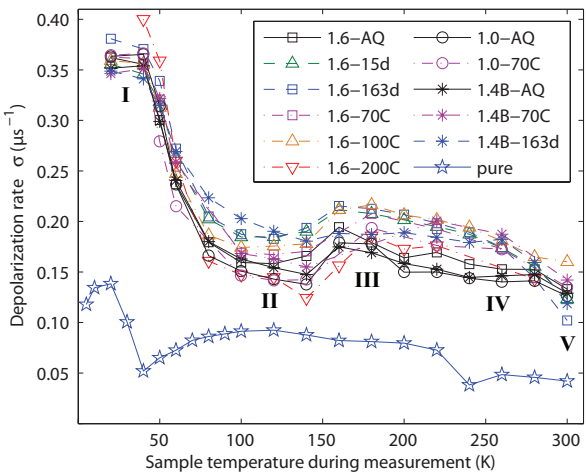

FIG. 3. (Color online) Muon depolarization rate in pure Al (99.99%) and Al–Mg–Si alloy conditions in Table I as a function of temperature. The fit errors are roughly as large as the markers.

V. RESULTS

The temperature dependence on the shape of the muon spin relaxation functions is quite similar for all the alloy conditions. As expected, pure aluminium is unique in this respect. Figure 2 shows typical relaxation functions for pure Al and an RT stored alloy condition. Although error bars are not shown, the measurement error increases toward longer times. This is due to poor statistics: Only a few muons survive as long as 25 μs, which is over 10 times the average muon lifetime. What best quantifies the curve shapes is the Gaussian fitting parameter σ, which is plotted for all conditions and measurement temperatures in Fig. 3.

Pure aluminium always has the lowest value of σ. The most pronounced feature of its temperature variation is a peak centered at about 20 K. The alloys also have high values of σ close to this peak, with relaxation func-

tions well described by the static KT function [see Eq. (4)]. In the temperature range of this study, σ shows a behavior in Al–Mg–Si alloys remarkably similar to the behaviors in 99.98% pure Nb in the range 11–77 K[10] and Zn-doped GaAs in the range 50–700 K.[5] The peaks are not expected to reflect the same types of defects in these very different materials.

Roman numerals mark the main features of the alloy curves in Fig. 3. The following observations can be drawn about differences between alloy conditions in the different regions:

- The 1.0% solute alloy has a lower σ value than the 1.6% solute alloy in all regions except at point **I**.
- At point **I**, The σ values are most similar for all conditions. The greatest deviation is the value for `1.6-200C`, which is higher than the average.
- At point **II**, σ is consistently ordered by heat treatment. From low to high values: As-quenched, 70–100°C annealed, RT stored. The 200°C annealed condition is the exception from this pattern. The minimum in σ is shifted to higher temperatures for the Mg–Si balanced `1.4B` conditions.
- Peak **III** is seen for all conditions except `1.4B-163d`. It is shifted to higher temperatures for the annealed samples.
- The curves for the as-quenched conditions are lower than the others from 180 K to 260 K. These, as well as `1.4B-163d`, have a high-temperature plateau at point **IV**.
- At point **V**, the RT stored conditions reach lower than all other conditions, while the order at point **II** is otherwise kept.

The best-fit relaxation functions simulated by the MC algorithm mostly lie within the measurement error of the experimental ones. To achieve this, a complicated temperature variation in the fitting parameters is required. Figure 4(a–c) shows the fitting parameters of 7 selected conditions for all measurement temperatures. We see that the temperature variation of σ in Fig. 3 is an effect of variations in all the parameters Δ, ν_t and ν_d. The least stable parameter is the fraction of initially trapped muons, p_0, which has the least effect on the relaxation function. Its variation is dominated by fluctuations around average values of $\approx 25\%$ for the alloys and $\approx 20\%$ for pure Al. It is not shown as it gives no additional information to help interpret the relaxation functions. Included in Fig. 4(d) is the estimated fraction of time a muon spends trapped in defects, f_t from Eq. 6.

The `1.6-200C` condition is the only one with a high-temperature heat treatment, which allows phases to be precipitated in the matrix. It was investigated by TEM, and was found to contain β'' needles[32] (concentration: 69000 $\mu\mathrm{m}^{-3}$, avg. length: 13 nm), and β' needles[33] (concentration: 400 $\mu\mathrm{m}^{-3}$, avg. length: 122 nm), giving a total precipitate volume fraction of 1.2%. The methodology used for this quantification is explained elsewhere.[27]

VI. DISCUSSION

Based on earlier studies, we have some conceptions about types and concentrations of defects in the alloy samples. Right after SHT, only point defects (single solute atoms and vacancies) are present, but we know that the clustering of solute atoms starts within minutes.[12,26] When the material is kept at temperatures between RT and 100°C, a high concentration ($\sim 10^6$ $\mu\mathrm{m}^{-3}$) of small clusters form[25,34] at a highly temperature-dependent rate. After 1000 minutes at 200°C, most clusters are dissolved, and the microstructure consists of the much larger precipitates observed by TEM as well as a dilute solid solution ($\approx 0.4\%$) of Mg and Si atoms. Whether muons diffuse into Al–Mg–Si precipitates and how this affects muon spin relaxation is unknown, but the results from condition `1.6-200C` is included for reference. The concentration of vacancies will decrease with storage/annealing time, but the rate of this decrease is unknown.

Most of the muon spin relaxation functions, some of which are shown in Fig. 2, have Gaussian-like shapes. No theory predicts this particular shape explicitly. It arises as a convolution of a constant function (fast diffusion) and a static KT function (trapping by defects). The significant depolarization (above $\sigma \approx 0.05$ $\mu\mathrm{s}^{-1}$) observed at most temperatures give clear signs of muon trapping in both pure Al and the Al alloys. Simulations help to further clarify the nature of this trapping in the different temperature regimes. They show that increased trapping does not always cause an increase in σ, in fact it can also have the opposite effect. We have made no attempt to explain the temperature variation of Δ on the basis of the local magnetic fields at different trapping sites.

The µSR temperature series results are discussed for three separate ranges of measurement temperatures.

A. Low temperature

The pure Al σ peak at 5–40 K has been observed earlier, for Al with 42 and 70 ppm Mn[35] and Al with 117 ppm Ag.[36] Its height was found to increase with the concentration of the trace elements, and its position along the temperature axis is influenced by the type of element. For Mn, the maximum is at 15 K, similar to what we measure in our sample with ≈ 100 ppm trace elements (possibly Fe, Ti, Zn, Cr, Mn, Cu and Zr). The peak is concurrent with an increased trapping rate, explaining the connection to trace element concentration.

Considering the pure aluminium results, we find it reasonable to assume that muons are trapped by free solute

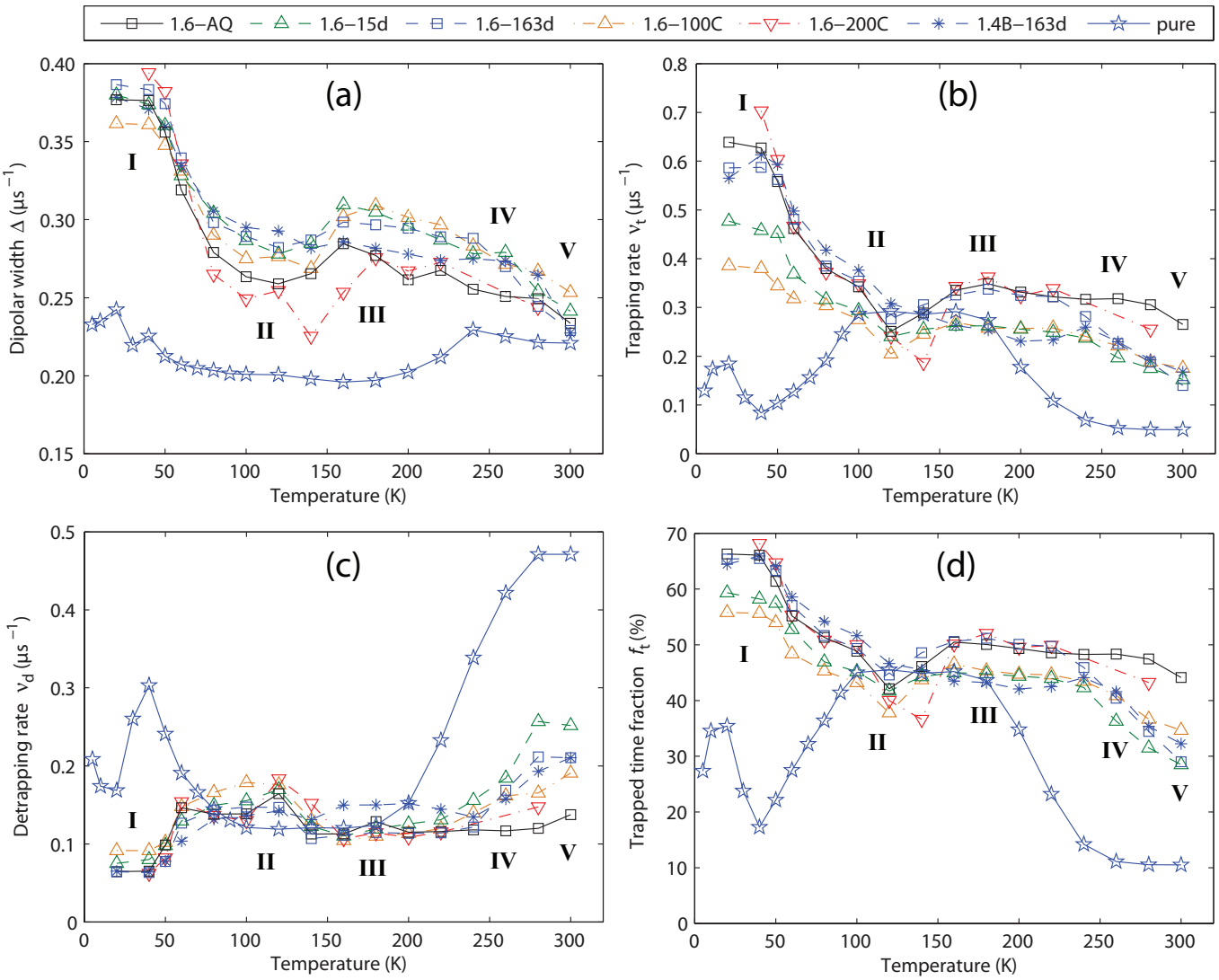

FIG. 4. (Color online) Temperature variation in the physical quantities obtained from fitting simulations to experimental relaxation functions. (a–c): Fitting parameters. (d): The fraction of time muons spend trapped, calculated from Eq. 6.

atoms at **I** in the alloy curves of Fig. 3. Figure 4(c) further shows a high trapping rate in the as-quenched alloys at this point. Annealing at 70–100°C reduces this rate, presumably via solute–solute bond formation. The trapping rate is also reduced by 15 days of RT storage, but increases again after 163 days. NA has been observed to give complicated long-time kinetics.[12] The most likely explanation to increased muon trapping by single solute atoms after long times is the dissolution of energetically unfavorable clusters.[25,34] The `1.6-200C` condition has the least amount of atoms in solid solution, but shows signs of even more trapping than in the as-quenched conditions. It is unclear whether this is an effect of its precipitate phases or other defects. For all alloy conditions, the low-temperature trapping sites are characterized by a dipolar width of $\Delta \approx 0.37\ \mu\text{s}^{-1}$.

B. Intermediate temperatures

The intermediate temperature σ peak at **III** is higher for conditions with more solute atoms and longer aging at temperatures between RT and 100°C, suggesting that it is caused by solute clusters/vacancy–solute complexes. From the simulation parameters in Fig. 4, we see both an elevated value of Δ and low detrapping rates in this area. For the Mg–Si-balanced condition `1.4B-163d`, the σ peak is near absent. In Fig. 4(c), we see that this coincides with a higher rate of detrapping. From APT studies, we know that this condition contains clusters that are less Mg-rich than the clusters in the `1.6` conditions.[25] A higher detrapping rate means that muons do not bind as tightly to the trapping sites, here assumed to be relatively Mg-poor clusters. This matter is subject to further study.

In light of the heat treatment-consistent differences in σ and Δ in Figs. 3 and 4(a), we propose that the whole

temperature region from **II** to **IV** is a joint trapping region for all possible configurations of Mg–Si–vacancy clusters. If this model is correct, it explains why the as-quenched conditions have an overall high trapping rate, as a high number of solute–vacancy and solute–solute pairs must form quickly to initiate the clustering process. The trapping sites have a dipolar with of $\Delta \approx 0.29\ \mu\text{s}^{-1}$ around peak **III**.

We have not found an explanation for the trapping peak reaching from 50 K to 240 K in the pure Al curves. Quantitative predictions are difficult for pure Al due to a slow muon depolarization, which makes the fitting parameters very sensitive to small variations in the relaxation functions. Regardless, wee see that the estimated trapping rate reaches the values of the alloy conditions within this range. The value of Δ stays roughly constant through all temperatures for pure Al, which means that the muon environment remains mostly unchanged.

C. High temperature

In an earlier experiment, we measured a decrease in σ with time when storing both pure Al and the 1.6% solute alloy at 300 K after quenching from SHT[37]. In pure Al, the only change during this storage is a decreasing concentration of vacancies. This decrease will lead to less muon trapping and a change in the depolarization rate. Vacancies are therefore assumed to trap muons near point **V**. In comparison with other types of defects, the concentration of vacancies is extremely low in all our conditions, and should only affect muons at such high temperatures, where the muon diffusion is fastest.

We suggest from the previous findings that vacancies are the dominant muon trapping defects in Al alloys near point **V**. This explains the high amount of trapping in the as-quenched samples in this region [see Fig. 4(b,d)], as these samples contain more vacancies than the RT stored and annealed conditions. The high-temperature annealed condition `1.6-200C` has a surprisingly high degree of trapping at **V**, although it is expected to have the least amount of vacancies. One suggested explanation is that precipitate phases can contain vacancies trapped during the precipitation process, and that these vacancies can also act as muon traps.

VII. CONCLUSION

We have conducted muon spin relaxation experiments on Al–Mg–Si alloys of three different compositions, with the following heat treatments: as quenched from solution heat treatment, with room temperature storage to give way for solute clustering and with annealing at 70–100°C to accelerate this clustering process. In certain ranges of measurement temperatures, we have found systematic deviations in depolarization rates when varying the composition and heat treatment. These deviations can be interpreted as signatures of different defects that provide muon trapping sites. We observe muon trapping by solute atoms at 20–50 K and by vacancies around 300 K. There are also strong indications of influence on the muon depolarization by more extended defects such as Mg–Si(–vacancy) complexes and precipitate phases, which are formed during heat treatment. Results from our simulations suggest that muons are trapped by Mg–Si clusters at intermediate temperatures (100–250 K). A procedure for quantification of such clusters would be valuable for our understanding of age hardening phenomena and for the ability to enhance alloy properties. Additional temperature series measurements will be conducted to further clarify the effects of solute clustering on muon depolarization in Al–Mg–Si alloys.

ACKNOWLEDGMENTS

This work was financially supported by The Research Council of Norway and Norsk Hydro via project no. 193619, The Norwegian–Japanese Al–Mg–Si Alloy Precipitation Project.

* sigurd.wenner@ntnu.no

[1] A. Lappas, K. Prassides, K. Vavekis, D. Arcon, R. Blinc, P. Cevc, A. Amato, R. Feyerherm, F. N. Gygax, and A. Schenck, Science **24**, 1799 (1995).
[2] C. Bernhard, J. L. Tallon, C. Niedermayer, T. Blasius, A. Golnik, E. Brücher, R. K. Kremer, D. R. Noakes, C. E. Stronach, and E. J. Ansaldo, Phys. Rev. B **59**, 14099 (1999).
[3] T. Lancaster, S. J. Blundell, D. Andreica, M. Janoschek, B. Roessli, S. N. Gvasaliya, K. Conder, E. Pomjakushina, M. L. Brooks, P. J. Baker, D. Prabhakaran, W. Hayes, and F. L. Pratt, Phys. Rev. Lett. **98**, 197203 (2007).
[4] K. Nagamine, F. L. Pratt, I. Watanabe, and E. Torikai, RIKEN Review **35**, 126 (2001).
[5] K. H. Chow, B. Hitti, R. F. Kiefl, R. L. Lichti, and T. L. Estle, Phys. Rev. Lett. **87**, 216403 (2001).
[6] R. L. Lichti, K. H. Chow, and S. F. J. Cox, Phys. Rev. Lett. **101**, 136403 (2008).
[7] W. Gauster, A. Flory, K. Lynn, W. Kossler, D. Parkin, C. Stronach, and W. Lankford, Journal of Nuclear Materials **69-70**, 147 (1978).
[8] K. W. Kehr, D. Richter, J. M. Welter, O. Hartmann, E. Karlsson, L. O. Norlin, T. O. Niinikoski, and A. Yaouanc, Phys. Rev. B **26**, 567 (1982).
[9] E. Sato, T. Hatano, Y. Suzuki, M. Imafuku, M. Sunaga, M. Doyama, Y. Morozumi, T. Suzuki, and K. Nagamine, Hyperfine Interactions **17**, 203 (1984), 10.1007/BF02065903.

[10] C. Boekema, R. H. Heffner, R. L. Hutson, M. Leon, M. E. Schillaci, W. J. Kossler, M. Numan, and S. A. Dodds, Phys. Rev. B **26**, 2341 (1982).

[11] C. Marioara, S. Andersen, J. Jansen, and H. Zandbergen, Acta Materialia **51**, 789 (2003).

[12] S. Wenner, C. D. Marioara, S. J. Andersen, and R. Holmestad, Int. J. Mater. Res. **103**, 948 (2012).

[13] K. Yamada, T. Sato, and A. Kamio, Mater. Sci. Forum **331–337**, 669 (2000).

[14] I. Kovaćs, J. Lendvai, and E. Nagy, Acta Metallurgica **20**, 975 (1972).

[15] F. De Geuser, W. Lefebvre, and D. Blavette, Phil. Mag. Lett. **86**, 227 (2006).

[16] C. D. Marioara, S. J. Andersen, T. N. Stene, H. Hasting, J. Walmsley, A. T. J. Van Helvoort, and R. Holmestad, Phil. Mag. **87**, 3385 (2007).

[17] A. Yaouanc and P. D. De Réotier, *Muon Spin Rotation, Relaxation, and Resonance: Applications to Condensed Matter*, International Series of Monographs on Physics (Oxford University Press, 2011).

[18] R. S. Hayano, Y. J. Uemura, J. Imazato, N. Nishida, T. Yamazaki, and R. Kubo, Phys. Rev. B **20**, 850 (1979).

[19] R. Kubo and T. Toyabe, in *Magnetic Resonance and Relaxation*, edited by R. Blinc (North-Holland, Amsterdam, 1967) p. 810.

[20] E. Holzschuh and P. F. Meier, Phys. Rev. B **29**, 1129 (1984).

[21] T. Hatano, Y. Suzuki, M. Doyama, Y. J. Uemura, T. Yamazaki, and J. H. Brewer, Hyperfine Interactions **17**, 211 (1984).

[22] T. R. Waite, Phys. Rev. **107**, 463 (1957).

[23] I. Z. Machi, S. H. Connell, M. Dalton, M. J. Sithole, K. Bharuth-Ram, S. F. J. Cox, and C. Baines, Diam. Relat. Mater. **13**, 909 (2004).

[24] T. Matsuzaki, K. Ishida, K. Nagamine, I. Watanabe, G. H. Eaton, and W. G. Williams, Nuclear Instruments and Methods A **465**, 365 (2001).

[25] M. Torsæter, H. S. Hasting, W. Lefebvre, C. D. Marioara, J. C. Walmsley, S. J. Andersen, and R. Holmestad, J. Appl. Phys. **108**, 073527 (2010).

[26] J. Banhart, M. D. H. Lay, C. S. T. Chang, and A. J. Hill, Phys. Rev. B **83**, 014101 (2011).

[27] C. Marioara, S. Andersen, H. Zandbergen, and R. Holmestad, Metallurgical and Materials Transactions A **36**, 691 (2005), 10.1007/s11661-005-0185-1.

[28] C. Marioara, H. Nordmark, S. Andersen, and R. Holmestad, Journal of Materials Science **41**, 471 (2006), 10.1007/s10853-005-2470-1.

[29] F. L. Pratt, Physica B: Condensed Matter **289–290**, 710 (2000).

[30] O. Hartmann, E. Karlsson, L. O. Norlin, T. O. Niinikoski, K. W. Kehr, D. Richter, J. M. Welter, A. Yaouanc, and J. Le Hericy, Phys. Rev. Lett. **44**, 337 (1980).

[31] "Webelements: the periodic table on the web," `http://www.webelements.com`.

[32] H. W. Zandbergen, S. J. Andersen, and J. Jansen, Science **277**, 1221 (1997).

[33] R. Vissers, M. van Huis, J. Jansen, H. Zandbergen, C. Marioara, and S. Andersen, Acta Materialia **55**, 3815 (2007).

[34] M. Torsæter, *Quantitative studies of clustering and precipitation in Al–Mg–Si(–Cu) alloys*, Ph.D. thesis, Norwegian University of Science and Technology, Department of Physics (2011).

[35] T. Niinikoski, O. Hartmann, E. Karlsson, L. Norlin, K. Kehr, D. Richter, J. Welter, J. Chappert, and A. Yaouanc, Physica B+C **108**, 879 (1981).

[36] O. Hartmann, E. Karlsson, B. Lindgren, E. Wäckelgård, D. Richter, R. Hempelmann, and J. M. Welter, Hyperfine Interactions **17**, 197 (1984).

[37] S. Wenner, K. Matsuda, K. Nishimura, J. Banhart, T. Matsuzaki, D. Tomono, F. L. Pratt, M. Liu, Y. Yan, C. D. Marioara, and R. Holmestad, in *13th International Conference on Aluminum Alloys*, edited by W. Heiland, A. D. Rollett, and W. Cassada (Wiley, 2012) pp. 37–42.